Alzheimer's Research & Therapy

RESEARCH

Open Access

Medial temporal lobe atrophy patterns in early-versus late-onset amnestic Alzheimer's disease

Anika Wuestefeld[1*], Alexa Pichet Binette[1], Danielle van Westen[2,3], Olof Strandberg[1], Erik Stomrud[1,4], Niklas Mattsson-Carlgren[1,5,6], Shorena Janelidze[1], Ruben Smith[1,4], Sebastian Palmqvist[1,4], Hannah Baumeister[7], David Berron[1,7], Paul A. Yushkevich[8], Oskar Hansson[1,4], Nicola Spotorno[1†] and Laura E.M. Wisse[2*†]

Abstract

Background The medial temporal lobe (MTL) is hypothesized to be relatively spared in early-onset Alzheimer's disease (EOAD). Yet, detailed examination of MTL subfields and drivers of atrophy in amnestic EOAD is lacking.

Methods BioFINDER-2 participants with memory impairment, abnormal amyloid-β and tau-PET were included. Forty-one amnestic EOAD individuals ≤65 years and, as comparison, late-onset AD (aLOAD, ≥70 years, $n=154$) and amyloid-β-negative cognitively unimpaired controls were included. MTL subregions and biomarkers of (co-) pathologies were measured.

Results AD groups showed smaller MTL subregions compared to controls. Atrophy patterns were similar across AD groups: aLOAD showed thinner entorhinal cortices than aEOAD; aEOAD showed thinner parietal regions than aLOAD. aEOAD showed lower white matter hyperintensities than aLOAD. No differences in MTL tau-PET or transactive response DNA binding protein 43-proxy positivity were found.

Conclusions We found evidence for MTL atrophy in amnestic EOAD and overall similar levels to aLOAD of MTL tau pathology and co-pathologies.

Keywords Tau-PET imaging, Amyloid-beta, MRI, Medial temporal lobe subregions, Aging, In vivo, Amnestic AD, Early-onset, Late-onset, Amygdala segmentation protocol, TPD-43

†Nicola Spotorno and Laura E.M. Wisse contributed equally to this work and share last authorship.

*Correspondence:
Anika Wuestefeld
anika.wuestefeld@med.lu.se
Laura E.M. Wisse
lemwisse@gmail.com
[1]Clinical Memory Research Unit, Department of Clinical Sciences Malmö, Lund University, Klinikgatan 28, Room C1103b, Lund SE-22242, Sweden
[2]Department of Diagnostic Radiology, Clinical Sciences, Lund University, Klinikgatan 13B, Lund SE-22242, Sweden
[3]Image and Function, Skåne University Hospital, Lund 22242, Sweden
[4]Memory Clinic, Skåne University Hospital, Malmö 20502, Sweden
[5]Department of Neurology, Skåne University Hospital, Lund 22242, Sweden
[6]Wallenberg Center for Molecular Medicine, Lund University, Lund 22184, Sweden
[7]German Center for Neurodegenerative Diseases (DZNE), 39120 Magdeburg, Germany
[8]Penn Image Computing and Science Laboratory (PICSL), Department of Radiology, University of Pennsylvania, Philadelphia 19104, USA

Background

Early-onset Alzheimer's disease (EOAD) is commonly defined by a clinical onset before the age of 65 years and is one of the most common types of early-onset neurodegenerative dementia [1]. It shares the presence of main neuropathological features, i.e., fibrillar amyloid-β (Aβ) and hyperphosphorylated tau, with late-onset AD (LOAD; age > 65), but clinical features and other characteristics tend to differ between EOAD and LOAD [1]. For example, there is evidence for less semantic memory impairment and a more aggressive course with more neurofibrillary tangle (NFT) pathology in EOAD compared to LOAD [1, 2].

While prior research has investigated clinical, genetic or pathological differences in EOAD vs. LOAD, for example [3–6], many studies define EOAD only by age of onset. Thus, various clinical phenotypes, such as amnestic or non-amnestic EOAD [7], have been grouped together as EOAD [1]. Due to this grouping, observed differences between EOAD vs. LOAD may not be applicable to all clinical phenotypes. For example, the medial temporal lobe (MTL) has previously been found to be relatively spared in EOAD compared to LOAD in several studies [8–10]. However, it is unclear if this applies to amnestic EOAD given the common grouping of clinical phenotypes. Moreover, fine-grained changes in MTL subfield atrophy patterns have not been investigated. MTL subfields are heavily involved in memory function [11] but subserve different functions [12, 13]. Additionally, the cytoarchitectonic and functionally different MTL subfields are differently affected in AD and other neurodegenerative diseases [14–16]. The involvement of the MTL in amnestic EOAD is not well characterized, therefore it is of importance to investigate whether the MTL is affected in amnestic EOAD and to what extent the atrophy pattern differs from the more common amnestic LOAD [17].

In addition to Aβ and NFT, co-pathologies are also common in AD [18] and can affect the clinical course of the disease as well as atrophy patterns in the brain [18–20]. Common AD co-pathologies, such as cerebrovascular disease (CVD) or transactive response DNA binding protein 43 (TDP-43) pathology often occur in the MTL [21, 22]. Therefore, MTL atrophy patterns in amnestic AD are likely partially influenced by the presence of such co-pathologies. It has been suggested that co-pathologies are common in EOAD, albeit less than in LOAD, and contribute substantially to cognitive impairment in EOAD [5]. However, it is unclear if this equally applies to all the phenotypes of EOAD including amnestic EOAD.

In this cross-sectional study we aim to investigate if MTL atrophy occurs in individuals with amnestic early-onset cognitive impairment (aEOAD). To this end, we aim to compare MTL subfield differences across aEOAD with the amnestic LOAD (aLOAD) group and with cognitively normal controls as reference. Secondary aims include (I) investigating similar comparisons for neocortical composite regions in order to establish whether potential differences between aEOAD and aLOAD groups are specific to the MTL, and (II) assessing if common co-pathologies are present in aEOAD vs. aLOAD, and in comparison to healthy controls. Lastly, we explore if MTL atrophy is associated with AD pathologies and co-pathologies in the aEOAD group. Exploratory analyses focus on (I) cognitive performance in aEOAD and (II) comparisons with non-amnestic EOAD and LOAD groups.

Methods

Participants

We included 534 cognitively impaired from a memory clinic setting and unimpaired participants from population-based studies in the city of Malmö [23] older than 50 years from the Swedish BioFINDER-2 study (NCT03174938) who underwent magnetic resonance imaging (MRI) and tau positron emission tomography (PET). The study was approved by the ethical review board in Lund, Sweden, and all study participants provided written informed consent.

Inclusion criteria for the amnestic EOAD (aEOAD) group, were (I) mild cognitive impairment (MCI, Mini-Mental State Examination (MMSE) ≥ 24) or AD (MMSE ≥ 20; see details in [23]), (II) 50–65 years of age, and who (III) were Aβ and tau positive accordingly to cerebrospinal fluid (CSF) Aβ42/Aβ40 ratio and tau-PET respectively, and (IV) performed 1.5 standard deviations below age- and education-based norms on the Alzheimer's Disease Assessment Scale-Cognitive subscale (ADAS-cog) delayed word list recall [24]. Additionally, patients between 65 and 70 years of age, who indicated their age of onset was before 65 on the Cognitive Impairment Questionnaire (CIMP-QUEST) and fulfilled all the other criteria were included as aEOAD. The amnestic LOAD group (aLOAD) included only patients with age ≥ 70 years while the other criteria were shared between aEOAD and aLOAD. The gap of five years between aEOAD and aLOAD was chosen to minimize the possibility that aEOAD cases were included in the aLOAD group. Additionally, in secondary analyses, we included non-amnestic EOAD (naEOAD) and LOAD (naLOAD) participants that had the same group definitions as aEOAD and aLOAD except that the non-amnestic groups performed within age- and education-based norms on the episodic memory test. We focused only on cases who were Aβ- and tau-positive to ensure that the observed memory or cognitive impairments were at least partly due to AD proteinopathies. Additionally, none

of the included participants met the clinical criteria for PCA or the logopenic variant of PPA.

Two control groups were included, one younger control group (YCU) for aEOAD and one older control group (OCU) for aLOAD, given the inherent age differences between the patient groups. The control groups were (I) cognitively unimpaired (CU), (II) Aβ negative, (III) performed within age- and education-based norms on the ADAS-cog delayed word list recall, and (IV) were selected with the same age range as respective aEOAD or aLOAD group.

Cerebrospinal fluid biomarkers

For a majority of the participants (n=514), CSF levels of Aβ42 and Aβ40 were measured with the Roche Elecsys platform (Roche Diagnostics International Ltd., Basel, Switzerland) as described previously by Hansson et al. [25]. For the remaining participants (n=11), Lumipulse G (Fujirebio, n=9) or Meso-Scale Discovery (MSD; n=2) assays, were used to quantify concentration of Aβ42 and Aβ40. All CSF handling followed a standardized protocol [26, 27]. To determine Aβ-positivity, a cut-off for CSF Aβ42/Aβ40 ratio was used with previously described thresholds obtained using Gaussian Mixture Modeling (Elecsys: 0.080; Lumipulse G: 0.072; MSD: <0.077) [23, 28, 29].

Cognitive assesment

Participants' cognitive functioning was estimated with the MMSE [30], the Alzheimer's Disease Assessment Scale-Cognitive Subscale (ADAS-Cog) delayed word list recall [24], animal fluency [31], Boston Naming Test-15 (BNT-15) [32], Trail-Making Test B [33], Symbol digit modalities test [34], and the visual object and space perception (VOSP) battery subtest cubes [35]. The scores were z-transformed using Aβ- cognitively unimpaired individuals under the age of 40 from BioFINDER-2 (n=99; MMSE>=26). These cognitive measures were chosen in order to capture various aspects of human cognition, such as memory, visuospatial functioning, language, and processing speed.

Imaging protocol

MRI

T1-weighted, T2-weighted, and Fluid attenuated inversion recovery (T2-weighted FLAIR) images were acquired on a Siemens MAGENTOM Prisma 3T scanner (Siemens Healthineers, Erlangen, Germany) with a 64-channel head coil. Whole brain T1-weighted images (Magnetization Prepared – Rapid Gradient Echo, MPRAGE) were acquired with the following parameters: in-plane resolution=1×1 mm^2, slice thickness=1 mm, repetition time (TR)=1900 ms, echo time (TE)=2.54 ms, flip-angle=9. Coronal T2-weighted images were acquired using a turbo spin echo sequence (in-plane resolution=.4x.4 mm^2, slice thickness=2 mm, TR=8240 ms, TE=52 ms, flip-angle=150°) with hippocampal orientation. Similarly, axial T2-weighted FLAIR images were acquired (TR=5000 ms, TE=393 ms, TA=4:37 min with the same resolution and field of view of the T1-weighted images).

Structural MRI processing and analysis

Using the Automated Segmentation of Hippocampal Subfields (ASHS) packages for T1- and T2-weighted MR images [36–39], MTL subregions were automatically segmented. To obtain hippocampal subfield volumes (Subiculum, cornu ammonis (CA) 1, dentate gyrus (DG)) the T2-weighted package was used [39]. Anterior and posterior hippocampus (HC), and MTL cortical thickness measures (entorhinal cortex (ERC), Brodmann area (BA) 35 (≈transentorhinal cortex), BA36, and parahippocampal cortex) were extracted using the T1-weighted MRI package. Whole amygdala volumes were extracted using ASHS from a new atlas for T1-weighted MRI updated with an amygdala label created following a newly developed protocol (see supplementary methods, sFig. S1–S10, sTable S1–S2). Volumes of hippocampal subregions and the amygdala were corrected for ICV using volume-to-ICV fractions.

De Flores and colleagues [40] suggested that the ratio between anterior HC and parahippocampal cortex (measured with T1-ASHS) as a promising marker to assess the presence of TDP-43 pathology in dementia cases with AD neuropathologic change and was previously validated against post-mortem data. They propose a cut-off of 693.44 for this marker, indicating the presence of TDP-43 pathology for individuals with a ratio below this cut-off. Following their approach, a ratio between anterior HC volume and parahippocampal cortical thickness was calculated after regressing out ICV for anterior HC and age for both measures and the above-mentioned cut-off was applied.

After applying FreeSurfer 6 (https://surfer.nmr.mgh.harvard.edu/) to the T1-weighted image to obtain mean cortical thickness estimates, the neocortex was parcellated into five composite regions based on the Desikan-Killiany atlas. Average cortical thickness was extracted from the five composite regions consisting of: the lateral temporal (superior, middle, and inferior temporal, banks of the superior temporal sulcus, transverse temporal, temporal pole), lateral parietal (postcentral, inferior and superior parietal, supramarginal), medial parietal (paracentral, isthmus, posterior cingulate, precuneus), frontal (superior frontal, rostral and caudal middle frontal, pars opercularis, pars triangularis, pars orbitalis, lateral and medial orbitofrontal, precentral, paracentral, frontal

pole), and occipital (cuneus, lateral occipital, lingual, pericalcarine) cortices.

As supplementary analyses, the Longitudinal Early-onset Alzheimer's Disease Study (LEADS) signature mean thickness, comprising primarily temporal and parietal regions, was calculated, see [41], and compared between groups.

All regions of interest were averaged across hemispheres. All regions of interest were z-scored to facilitate comparisons between the measures using Aβ- cognitively unimpaired individuals under the age of 40 from BioFINDER-2 (n=99; MMSE>=26) as reference group.

[^{18}F]RO948 tau-PET

Tau-PET scans were acquired with a digital GE Discovery MI Scanner (General Electric Medical Systems). Tau-PET was performed 70–90 min post-injection of ~370 MBq of [^{18}F]RO948. Details of the PET reconstruction have been published previously [42]. The Swedish Medical Products Agency and the local Radiation Safety Committee at Skåne University Hospital, Sweden approved the PET imaging.

Tau-PET processing and analysis

Standardized uptake value ratios (SUVR) were calculated using an inferior cerebellar reference region for [^{18}F]RO948-PET (tau-PET) [43]. Using the geometric transfer matrix method [44], partial volume correction (PVC) was performed. See Leuzy et al. [42] for a detailed description of our processing pipeline.

[^{18}F]RO948-PET positivity was defined using a previously defined cut-off of a SUVR>1.362 [42] based on Gaussian Mixture Modeling in the temporal meta-ROI corresponding to Braak I-IV [45].

Tau-PET uptake was measures in two early regions (I) a composite MTL region from ASHS comprising ERC and BA35 from ASHS and (II) the amygdala from ASHS. The decision to use only ERC and BA35 was based on two aspects: (I) it reduces the potential bias caused by off target binding that typically occur around the hippocampus, (II) ERC and BA35 typically show the earliest accumulation of cortical tau pathology [14]. Using clusters previously defined with an event-based modelling (EBM) approach, see [46], tau-PET composite measures were calculated for four EBM-based regions of interest (lateral temporal, parietal, frontal, occipital/motor), that match the neocortical composite regions. Lastly, a composite tau-PET SUVR was calculated for the LEADS signature [41].

White matter hyperintensity volume processing and analysis

Using FreeSurfer 7.2 Sequence Adaptive Multimodal SEGmentation (SAMSEG) functionality [47, 48], white matter hyperintensities (WMH) were segmented from the T2-weighted FLAIR sequence. Whole brain WMH volumes were calculated per participant, corrected for ICV (using volume-to-ICV fractions) and log-transformed. This measure was used for primary analyses. Due to the distribution of the data (many participants with very low values), WMH volumes were also split into low/high based on median-split and used in sensitivity analyses.

Statistical analyses

Analyses were performed in R 4.0.2 [49]. All p-values were controlled for the false discovery rate (FDR, Benjamini–Hochberg procedure). P-values were considered statistically significant at $p<.05$. Group comparisons did not by default include age as a covariate, since the AD groups are defined by age. Only comparisons between controls and respective AD groups included age as covariate in sensitivity analyses.

Differences in demographic variables were tested using t-tests or chi-square tests. We examined group differences between aEOAD and aLOAD with respective controls and with each other for demographics and cognitive measures.

For our main aim, we examined group differences between aEOAD and aLOAD with respective controls and with each other for volume/thickness of the MTL regions of interest (3 comparisons) using one-way ANCOVAs along with post-hoc Tukey's HSD Test for multiple comparisons, including sex as covariate. We also investigate the interaction between age group (young vs. old) and diagnosis (CU vs. AD) in a linear regression model for each region in order to investigate if morphological metrics (i.e. volume or thickness) are differently affected by aging and disease state.

In addition, we characterized the aEOAD and aLOAD groups further by examining group differences between aEOAD and LOAD with respective controls and with each other. This analysis was conducted, first, for the thickness of neocortical composite regions. We used ANCOVA to investigate group differences and performed linear regression models for each region with the interaction between age and diagnosis. Second, groups were compared for all biomarkers of AD- and co-pathologies. We used ANCOVA for continuous outcomes and logistic regression for categorical variables to assess group differences for the positivity on the aHC/PHC ratio (MRI-based proxy for potential TDP-43 positivity), as well as binarized WMH volume (low vs. high). In all analyses, sex was included as covariate.

As sensitivity analyses, age was included as covariate for comparisons between AD groups and controls. Second, for comparisons of AD- and co-pathologies, we included also CSF Aβ42/Aβ40 ratio as a covariate to investigate if differences between all group comparisons

were influenced by Aβ. Additional analyses additionally investigated group differences between aEOAD and aLOAD for the both LEADS signature thickness and tau-PET SUVR.

Secondary analyses

As exploratory analyses, we aim to investigate if different pathologies could explain lower region of interest volume/thickness within the aEOAD group. To this end, we performed linear regressions predicting region of interest volume/thickness using biomarkers of AD- and co-pathologies including age and sex as covariates.

We explored group comparisons for cognitive performance (ADAS-cog delayed word recall, animal fluency, trail-making test B, VOSP cube, BNT-15). ANOVAs were used including sex and education as covariates. We also explore if differences in volume/thickness were associated with cognitive performance within the aEOAD group, including education level, age, and sex as covariates.

In a final step, we also explored group comparisons for the amnestic and non-amnestic EOAD (aEOAD vs. naEOAD) and LOAD (aLOAD vs. naLOAD) groups. The non-amnestic individuals are included only in this section of the secondary analyses.

Results

Demographics

The sample consisted of 534 older adults (56.9% female, mean age 69.2, mean education 12.8 years, 47.4% were *APOE-ε4* carriers). The demographics of the aEOAD ($n=41$) and aLOAD ($n=154$) groups as well as the two control groups are shown in Table 1. The demographics of the non-amnestic AD groups (naEOAD: $n=7$, naLOAD: $n=16$) are shown in sTable S3. Comparing aEOAD vs. LOAD, no differences in sex, education, MMSE, or *APOE* status were observed. A significant difference between aLOAD and respective controls was observed for sex (lower proportion of males in the AD groups), and, as expected, *APOE* status (higher proportion of *APOE-ε4* carriership in the AD groups). There was no difference in diagnosis between aEOAD and aLOAD groups. Despite selecting amnestic AD patients and controls from the same age range, age was statistically significantly different between amnestic AD groups and the respective controls, likely due to non-normal distributions within the AD groups. While the age difference is likely negligible due to same age range and overlapping mean and standard deviations of AD groups with controls, we did adjust for age in sensitivity analyses when comparing the amnestic AD groups to their respective control groups.

Amnestic EOAD shows medial temporal lobe subfield involvement

A statistically significant difference in mean value was found for all MTL regions of interest for both aEOAD and aLOAD compared to respective control groups (Fig. 1, supplementary results sTable S4). The biggest differences comparing aEOAD with controls were observed in amygdala, BA35, and total hippocampus (z-score mean differences = 1.89, 1.70, -1.68 respectively, all $p<.001$). The biggest differences comparing aLOAD with controls were observed in entorhinal cortex, amygdala, and total

Table 1 Characteristics of the amnestic EOAD and LOAD groups and respective controls

	YCU	OCU	aEOAD	aLOAD	Total	*p*-value YCU-aEOAD	*p*-value OCU-aLOAD	*p*-value aEOAD-aLOAD
N	188	151	41	154	534	-	-	-
Diagnosis						-	-	0.713
CU	188 (100)	151 (100)	0 (0)	0 (0)	339 (63.5)			
MCI	0 (0)	0 (0)	16 (39.0)	65 (42.2)	81 (15.2)			
AD	0 (0)	0 (0)	25 (61.0)	89 (57.8)	114 (21.3)			
Sex (female)	103 (54.8)	99 (65.5)	20 (48.8)	82 (53.2)	304 (56.9)	0.485	**0.029**	0.611
Age	58.6 ± 4.89	77.3 ± 3.38	61.0 ± 4.82	76.2 ± 3.92	69.2 ± 9.76	**0.005**	**0.008**	-
Range	51.0–69.0	70.3–85.0	50.9–69.4[a]	70.1–85.1	50.9–85.1			
Education (years)	13.2 ± 3.12	12.4 ± 3.74	14.1 ± 3.33	12.5 ± 4.79	12.8 ± 3.86	0.116	0.816	0.052
Missing	2 (1.1)	0 (0.0)	1 (2.4)	6 (3.9)	9 (1.7)			
***APOE-ε4*allele+**	85 (45.2)	29 (19.2)	25 (61.0)	114 (74.0)	253 (47.4)	0.066	**< 0.001**	0.116
CSF Aβ42/40+[b]	0 (0.0)	0 (0.0)	41 (100)	154 (100)	195 (36.5)	-	-	-
MMSE	29.2 ± 0.92	28.8 ± 1.20	24.6 ± 3.22	24.4 ± 2.53	27.3 ± 2.87	< 0.001	< 0.001	0.622

Continuous variables are displayed as mean ± SD. Categorical variables are displayed as n (%). Bold *p*-values are statistically significant at $p < 0.05$

Abbreviations Aβ = amyloid-beta; AD = Alzheimer's disease; aEOAD = amnestic early-onset cognitive impairment, aLOAD = amnestic late-onset cognitive impairment; APOE = apolipoprotein E; CU = cognitively unimpaired; CSF = cerebrospinal fluid; MCI = mild cognitive impairment; MMSE = Mini-Mental State Examination; OCU = older cognitively unimpaired controls; SD = standard deviation; YCU = younger cognitively unimpaired controls

[a] individuals who reported an age-of-onset under 65 were included in the EOAD group. [b] Aβ positivity: <0.08 on CSF Aβ42/40 ratio. The demographic information of the non-amnestic EOAD and LOAD individuals can be found in sTable S3 and are not included in the total of this table

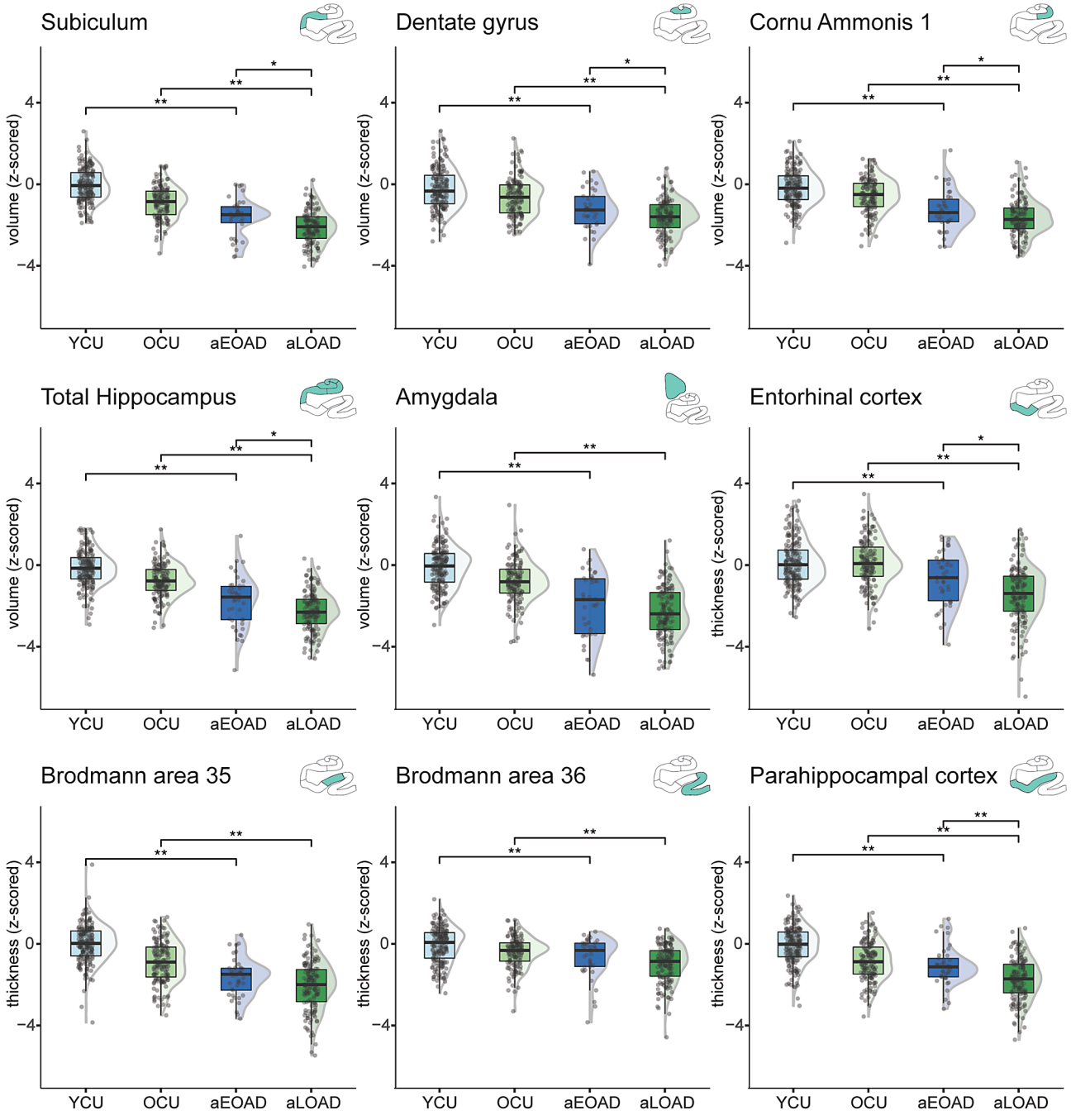

Fig. 1 aEOAD and aLOAD group differences and to respective controls in medial temporal lobe subfield volume/thickness. The figure shows the group comparisons for all medial temporal lobe subfield measures, indicating significant differences of amnestic AD groups to respective controls, but limited differences between aEOAD and aLOAD. Separate ANOVAs were performed for each comparison. Post-hoc comparisons focused on three group differences: young controls vs. aEOAD, older controls vs. aLOAD, and aEOAD vs. aLOAD. Significant differences are shown using FDR-corrected p-values; *=p_{FDR} < .05; **=p_{FDR} < .001. The ROI measures were z-scored based on young cognitively unimpaired individuals (< 40, CSF Aβ42/40 negative). All analyses included sex as a covariate. Results for the neocortical regions are included in the supplementary information. Non-amnestic individuals were not considered for these analyses. *Abbreviations*: aEOAD = amnestic early-onset Alzheimer's Disease; aLOAD = amnestic late-onset Alzheimer's disease; OCU = older cognitively unimpaired controls; YCU = younger cognitively unimpaired controls

hippocampus (mean differences = 1.59, 1.55, 1.55 respectively, all p < .001). These results indicate similar atrophy patterns across the medial temporal lobe (sFig. S11) between aEOAD and aLOAD, which was also confirmed by the lack of statistically significant interactions between age and diagnosis (sTable S5). The only exception was ERC where larger atrophy in aLOAD appears and the interaction between age group and diagnosis was

significant (sTable S5). These results contrast with previous reports which suggested limited involvement of the MTL in aEOAD (see sTable S4). Including age as covariate did not change these results (see sTable S4).

Focusing on the differences between aEOAD and aLOAD, significantly lower volume or thickness was found in aLOAD compared to aEOAD in five regions: subiculum (mean difference=0.50, p_{FDR}=0.004), dentate gyrus (mean difference=0.38, p_{FDR}=0.042), Cornu Ammonis 1 (mean difference=0.39, p_{FDR}=0.042), entorhinal (mean difference=0.78, p_{FDR}=0.003), and parahippocampal cortex (mean difference=0.68, p_{FDR}<0.001). Also, total hippocampal volume differed between aEOAD and aLOAD (mean difference=0.50, p_{FDR}=0.011, Fig. 1, sTable S4).

Further characterization of amnestic EOAD and LOAD

Neocortical thickness differences in amnestic EOAD vs. LOAD for frontal and lateral temporal cortices

As additional analyses, potential differences in thickness of neocortical regions in aEOAD and aLOAD were investigated. When comparing AD groups with their respective controls, a statistically significant difference was found for all neocortical regions of interest (sFig. S12A). The pattern of atrophy between aEOAD and aLOAD compared with respective controls was similar for all regions except for lateral and medial parietal cortices, for which the interaction between age group and diagnosis was also significant, indicating more prominent atrophy in the aEOAD group (sFig. S12B). Additionally, significantly lower lateral temporal and frontal thickness was found in LO- compared to aEOAD (p_{FDR}=0.031, 95%-C.I.=[-0.728, -0.051] and p_{FDR}=0.014, 95%-C.I.=[-0.841, -0.116] respectively; sFig. S12).

Lastly, comparisons of thickness in the LEADS signature were performed. Both aEOAD and aLOAD showed significantly thinner thickness compared to controls but no differences between aEOAD and aLOAD (see sFig. S13).

Amnestic EOAD shows a similar AD- and co-pathology burden as amnestic LOAD compared to controls

In a next step, we investigated potential differences in aEOAD vs. aLOAD with regards to common pathologies often accumulating in and related to MTL atrophy. Comparing AD groups with respective controls, a statistically significant difference in mean value was found for most AD pathologies and co-pathologies, indicating significantly higher pathology burden in the AD groups (MTL tau-PET SUVR, aHC/PHC ratio as TDP-43 proxy, CSF Aβ42/Aβ40 ratio; Fig. 2, supplementary material sTable S6). Only the total volume of WMH did not differ significantly between aLOAD and controls (p_{FDR}=0.085). The results remained consistent when including age as covariate, except that a significant difference between aLOAD and controls was found for WMH (p_{FDR}=0.033, see supplementary results sTable S7).

Focusing on the differences between aEOAD and aLOAD, we found a statistically significant higher mean value for WMH in aLOAD compared to aEOAD (p_{FDR}<0.001, 95%-C.I.=[0.056, 0.170]; Fig. 2; see supplementary sTable S6 and sFig. S14 for results using a dichotomized white matter hyperintensity measure). No differences in biomarkers of AD (MTL tau-PET and CSF Aβ42/Aβ40 ratio) were observed between aEOAD and aLOAD (Fig. 2). Additionally, no differences between aEOAD and aLOAD were observed in the proportion of positivity for MRI-based proxy of TDP-43 pathology (Fig. 2, sTable S6). Results of these group comparisons did not change when accounting for CSF Aβ42/Aβ40 ratio in the models.

Comparisons of tau-PET uptake in all four neocortical composite regions and the LEADS signature show higher uptake in AD groups compared to controls and aEOAD showed a significantly higher tau-PET uptake in these neocortical composite regions compared to aLOAD (see sTable S6, sFig. S13 and sFig.S15).

Associations between AD- and co-pathologies and atrophy in amnestic EOAD

In order to explore potential associations between AD- and co-pathologies and the structural measures, we focused only on the regions of interest which showed significant differences between aEOAD and aLOAD (total hippocampus (including subiculum, dentate gyrus, and cornu ammonis 1), entorhinal, parahippocampal; see sFig. S16).

Only the proxy of the presence of TDP-43 pathology was significantly associated with smaller total hippocampal volumes (std. β=-0.63, p_{FDR}<0.001). However, this association may be due to the definition of the measure considering the anterior hippocampus constitutes a large proportion of total hippocampal volume.

Cognitive performance in amnestic EOAD

Exploring group differences in cognitive performance, worse performance of the AD groups compared to respective controls was observed for all cognitive measures, while lower verbal fluency and naming abilities in aLOAD compared to aEOAD were observed (see sTable S8). No significant associations between MTL atrophy and performance on cognitive domains dependent on the MTL (episodic memory, naming, semantic fluency) were found for the aEOAD group (see sFig. S17).

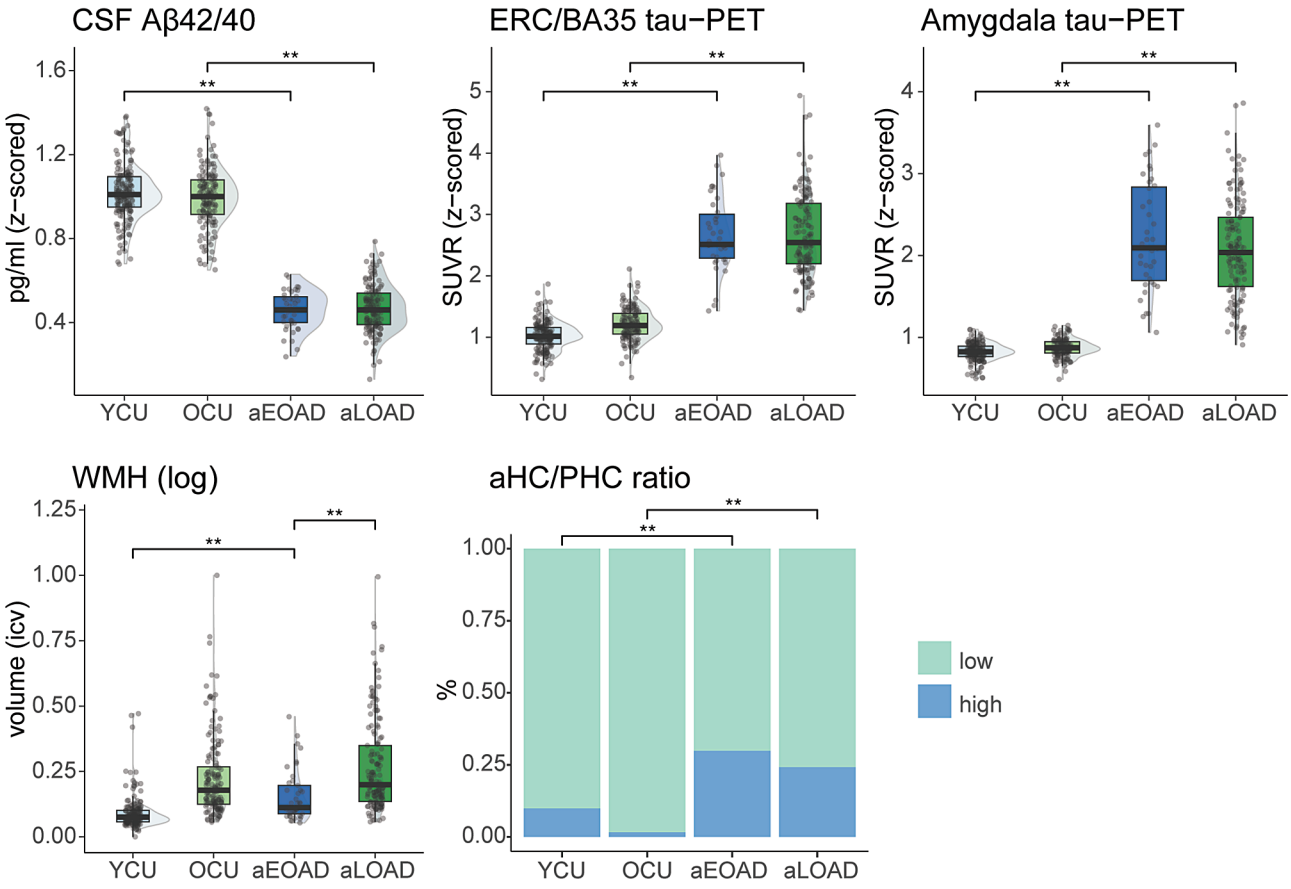

Fig. 2 aEOAD and aLOAD group differences and to respective controls in AD pathologies and co-pathologies. The figure shows the group comparisons for all AD and non-AD pathologies, indicating significant differences of amnestic AD groups to respective controls, but only a significant difference in WMH volume between aEOAD and aLOAD. Separate ANOVAs were performed for each pathology. Post-hoc comparisons focused on three group differences: younger controls vs. EOAD, older controls vs. aLOAD, and aEOAD vs. aLOAD. Significant differences are shown using FDR-corrected p-values; *=p_{FDR} < .05; **=p_{FDR} < .001. aHC/PHC ratio is an approximation of TDP-43 pathology. All analyses included sex as a covariate. Non-amnestic individuals were not considered for these analyses. *Abbreviations*: Aβ = amyloid-beta; aHC/PHC ratio = ratio of anterior hippocampus and parahippocampal cortex; aEOAD = amnestic early-onset Alzheimer's Disease; aLOAD = amnestic late-onset Alzheimer's disease; CSF = cerebrospinal fluid; PET = positron emission tomography; SUVR = standardized uptake value ratio; OCU = older cognitively unimpaired controls; WMH = white matter hyperintensities; YCU = younger cognitively unimpaired controls

Comparison between amnestic and non-amnestic EOAD and LOAD

Demographic information on the non-amnestic AD (naEOAD: n=7; naLOAD: n=16) are provided in the supplementary material (sTable S1). Both amnestic AD groups showed lower MTL, but not neocortical, volume/thickness compared to non-amnestic AD (see sTable S9, sFig. S18– S19). Subiculum volume and BA35 thickness were significantly smaller in amnestic vs. non-amnestic EOAD (see sTable S9, sFig. S18). The amnestic, compared to the non-amnestic AD groups showed higher amygdala tau-PET uptake. Non-amnestic LOAD showed larger WMH volumes compared to amnestic LOAD (see sTable S10, sFig. S20). Additionally, no difference in cognitive performance was observed between amnestic and non-amnestic AD groups (see sTable S10, sFig. S20). Including age as covariate did not change these results (sTables S11+ S12).

Discussion

The major aim of this cross-sectional study was to investigate if the MTL is affected in amnestic EOAD by comparing this group to amnestic LOAD atrophy patterns and respective controls in fine-grained MTL subregions from a highly characterized cohort and using a new reliable automated whole amygdala segmentation. In contrast with previous reports [8–10], amnestic EOAD, as well as amnestic LOAD, showed significantly smaller volumes of MTL regions compared to controls. Amnestic LOAD, compared to amnestic EOAD, was found to have smaller volumes/thickness in the MTL only for hippocampus, entorhinal and parahippocampal cortex, and in the neocortical regions in lateral temporal and

frontal cortex. To further characterize the AD groups, we focused on biomarkers of AD and non-AD pathologies that often affect the MTL. The amnestic EOAD grouped showed higher neocortical tau-PET uptake but lower WMH burden, compared to amnestic LOAD. However, no differences were observed for our proxy of TDP-43. Lastly, the proxy of TDP-43 positivity was associated with smaller hippocampal volumes indicating a potential involvement in driving atrophy in this region.

Our results show that the MTL is affected in amnestic AD, irrespective of age. This may seem in contrast with previous reports showing evidence of relative sparing of the MTL in EOAD [1, 50, 51]. However, since prior studies commonly grouped all EOAD subtypes together, except e.g [52]. it is possible that MTL atrophy in these studies was concealed by other phenotypes. The importance of the MTL in memory function [13], suggests that an amnestic type of AD should be associated with MTL atrophy, regardless of age of onset, a notion that is supported by our findings.

Even though we observed lower MTL thickness in amnestic EOAD when comparing with controls, amnestic LOAD still shows more atrophy within the MTL (e.g., lower thickness in entorhinal cortex compared to aEOAD). This may be due to several reasons. First, there may be non-specific aging effects on these cortical structures leading to more atrophy in the older patient group. Second, for some individuals, pathologies may have a longer duration of accumulation in these regions, potentially exerting an effect on structure for a longer duration resulting in more atrophy. Previous reports of increased parietal atrophy in EOAD [1] were supported in our amnestic EOAD sample, given the significant interaction between age and diagnosis for parietal regions, indicating more prominent atrophy in the amnestic EOAD group than in amnestic LOAD. Additionally, we did observe higher levels of tau-PET uptake in parietal regions in the amnestic EOAD group, which may potentially contribute to the more pronounced atrophy in this region.

In comparison to respective controls, the amnestic AD groups show similar significant increased frequency or severity in the investigated co-pathologies. The only exception was observed for WMH which were increased in amnestic EOAD, but not in amnestic LOAD, where the results were more inconsistent. The fact that the amnestic EOAD group shows a similar level of co-pathologies as amnestic LOAD may be due to faster accumulation of pathologies, such as tau, but could also reflect a lack of resilience to pathologies. The mechanisms behind the presence of these co-pathologies for amnestic EOAD despite younger age remains to be elucidated.

It is of interest that no differences between amnestic EOAD and LOAD were found for a common co-pathology, the proxy of TDP-43 pathology. Previously, it has been reported significantly less TDP-43 proteinopathy in EOAD compared to LOAD [5]. This was not replicated in the present study using a proxy of TDP-43 based on the observed anterior to posterior gradient of TDP-43 occurrences in the MTL [40]. It is possible that the proxy, established in an autopsy cohort, does not replicate to our cohort, even though a similar cut-off was found when replicating it in our cohort (693 vs. 645) using Gaussian mixture modeling without postmortem validation. The fact that no difference between AD groups was observed could, however, also be due to a smaller sample size compared to what the study by Spina and colleagues [5] included and the indirect nature of our measure for presence of TDP-43. Nevertheless, we did find that our measure of TDP-43 positivity was associated with lower hippocampal volume in the amnestic EOAD group, indicating a potential driving factor of atrophy specific to aEOAD, which must be replicated in a larger sample.

Previous studies have reported a higher burden of AD pathology in amnestic EOAD compared to LOAD [2, 5, 53]. We found that amnestic EOAD shows more neocortical tau pathology while presenting similar levels of MTL tau to amnestic LOAD. Our results are, thus, in line with the notion of EOAD showing a more aggressive disease progression with faster cognitive decline and accumulation of pathology [1] and previous observations of higher levels of tau accumulation in younger individuals [54]. This adds to the existing literature since evidence for this faster progression has not been investigated specifically in an amnestic EOAD sample. The null results regarding our analyses associating co-pathologies with MTL structural measures in amnestic EOAD are likely due to limited power. Lastly, while EOAD is thought to be characterized by a steeper cognitive decline over time [55], we found that the aLOAD sample showed worse performance in semantic fluency and picture-naming abilities compared to aEOAD. Nevertheless, a longitudinal investigation of these factors should be conducted in a larger sample and employing a more fine-grained neuropsychological assessment.

Strengths and limitations

Strengths of the current study include the fine-grained investigation of MTL subfields, the use of a highly characterized cohort with various biomarkers of (co-)pathologies available, and the focus on amnestic EOAD as a separate group. Additionally, a new reliable automated segmentation for the whole amygdala is presented. However, the study also presents some limitations. First, the sample size of the amnestic EOAD group is relatively small. While this corresponds to the lower proportion of EOAD in the general population [56], it results in lower statistical power. Thus, future studies should investigate a larger sample of amnestic EOAD. Second, the cross-sectional nature of the study does not allow us to draw conclusions about potential more

aggressive courses or larger atrophy rates between groups. Third, cognitively unimpaired participants are enriched for *APOE-ε4* allele carriership in the BioFINDER-2 study [23] and, in this study, the younger control group showed a larger percentage of *APOE*-positivity. A replication of this study is, thus, needed, using a control group not enriched for *APOE* status.

Conclusions

In summary, we found a largely similar MTL atrophy pattern in amnestic EOAD compared to LOAD in this cross-sectional study. Interestingly, besides lower white matter hyperintensity volumes and higher neocortical tau PET in amnestic EOAD compared to amnestic LOAD, no differences in other AD- and co-pathologies, such as MTL tau-PET, and our proxy of TDP-43 were observed between amnestic EOAD and LOAD. These results suggests that the driving mechanisms of the amnestic symptoms in both groups might be largely similar and resulting in similar atrophy patterns within the MTL.

Abbreviations

Aβ	Amyloid-beta
AD	Alzheimer's disease
ADAS-cog	Alzheimer's Disease Assessment Scale-Cognitive subscale
aEOAD	Amnestic early-onset Alzheimer's Disease
aHC	Anterior Hippocampus
aLOAD	Amnestic late-onset Alzheimer's Disease
AMY	Amygdala
ANCOVA	Analysis of covariance
APOE	Apolipoprotein E
ASHS	Automated Segmentation of Hippocampal Subfields
BA35	Brodmann area 35 (≈transentorhinal cortex)
BNT	Boston Naming Test – 15 items
CA1	Cornu ammonis 1
C.I	Confidence interval
CSF	Cerebrospinal fluid
CU	Cognitively unimpaired
ERC	Entorhinal cortex
EBM	Event-based modeling
FL	Frontal cortex
HC	Hippocampus
LT	Lateral temporal
LP	Lateral parietal
MCI	Mild cognitive impairment
MMSE	Mini-Mental State Examination
MP	Medial parietal
MRI	Magnetic resonance imaging
MTL	Medial temporal lobe
NFTs	Tau neurofibrillary tangles
OCU	Older cognitively unimpaired controls
OL	Occipital cortex
PET	Positron emission tomography
pHC	Posterior Hippocampus
PHC	Parahippocampal cortex
SD	Standard deviation
SUVR	Standardized uptake value ratio
SDM	Symbol digit modalities test
TDP-43	Transactive response DNA binding protein 43
TMT-B	Trail-Making Test B
VOSP Cube	Visual object and space perception battery subtest cubes
WMH	White matter hyperintensities
YCU	Younger cognitively unimpaired controls

Supplementary Information

The online version contains supplementary material available at https://doi.org/10.1186/s13195-024-01571-z.

Supplementary Material 1

Supplementary Material 2

Acknowledgements

We would like to acknowledge all the BioFINDER team members as well as participants in the study and their family members for their dedication. This study was supported by MultiPark - A Strategic Research Area at Lund University.

Author contributions

A.W., O.H., N.S., and L.E.M.W., designed the study. A.W. performed the analyses and data interpretations under the supervision of O.H., A.B.P., N.S., L.E.M.W. The manuscript was drafted by A.W. All authors contributed to preparation and critical review of the manuscript. O.H., S.J., S.P., E.S. R.S., H.B., D.B., P.A.Y., and N.M.C collected the clinical data and/or coordinated/performed biomarker quantifications and/or contributed to processing of the imaging data.

Funding

This study was supported by MultiPark - A Strategic Research Area at Lund University. Additionally, this work was supported by project grants from NIA (R01-AG070592, R01-AG069474, RF1-AG056014), the Swedish Research Council (2022 – 00900), Alzheimerfonden (AF980872, AF993465) and the Crafoord foundation (20210690).
The BioFINDER-2 study was supported by the European Research Council (ADG-101096455), Alzheimer's Association (ZEN24-1069572, SG-23-1061717), GHR Foundation, Swedish Research Council (2022 – 00775, 2018–02052, 2021–02219), ERA PerMed (ERAPERMED2021-184), the Knut and Alice Wallenberg foundation (2022 – 0231), the Strategic Research Area MultiPark (Multidisciplinary Research in Parkinson's disease) at Lund University, the Swedish Alzheimer Foundation (AF-980907, AF-980832, AF-994229), the Swedish Brain Foundation (FO2021-0293, FO2022-0204, FO2023-0163), The Parkinson foundation of Sweden (1412/22), Familjen Rönnströms Stiftelse (FRS-0003), WASP and DDLS Joint call for research projects (WASP/DDLS22-066), the Cure Alzheimer's fund, the Konung Gustaf V: s och Drottning Victorias Frimurarestiftelse, the Skåne University Hospital Foundation (2020-O000028), Regionalt Forskningsstöd (2022 – 1259) and the Swedish federal government under the ALF agreement (2022-Projekt0280, 2022-Projekt0107). The precursor of ^{18}F-flutemetamol was sponsored by GE Healthcare. A.P.B. is supported by a postdoctoral fellowship from the Fonds de recherche en Santé Québec (298314).The funding sources had no role in the design and conduct of the study; in the collection, analysis, interpretation of the data; or in the preparation, review, or approval of the manuscript.
Open access funding provided by Lund University.

Data availability

Pseudo-anonymized data from BioFINDER-2 will be shared on request from a qualified academic investigator for the sole purpose of replicating procedures and results presented in the article and as long as data transfer is in agreement with EU legislation on the general data protection regulation and decisions by the Swedish Ethical Review Authority and Region Skåne, which should be regulated in a material transfer agreement.

Declarations

Ethics approval and consent to participate

The study was approved by the Regionala Etiksprövningsnämnden i Lund (regional ethical review board in Lund), Sweden, and all study participants provided written informed consent in accordance with the Declaration of Helsinki.

Consent for publication

Not applicable.

Competing interests

A.W., A.P.B., H.B., E.S., O.S., D.W., N.M.-C, N.S., P.A.Y., and L.E.M.W. have nothing to declare. D.B. is co-founder of neotiv GmbH. R.S. has received a speaker fee from Roche. S.P. has acquired research support (for the institution) from ki elements / ADDF and Avid. In the past 2 years, he has received consultancy/speaker fees from Bioartic, Biogen, Esai, Lilly, and Roche. O.H. has acquired research support (for the institution) from AVID Radiopharmaceuticals, Biogen, C2N Diagnostics, Eli Lilly, Eisai, Fujirebio, GE Healthcare, and Roche. In the past 2 years, he has received consultancy/speaker fees from AC Immune, Alzpath, BioArctic, Biogen, Bristol Meyer Squibb, Cerveau, Eisai, Eli Lilly, Fujirebio, Merck, Novartis, Novo Nordisk, Roche, Sanofi and Siemens.

Received: 16 May 2024 / Accepted: 4 September 2024
Published online: 16 September 2024

References

1. Mendez MF. Early-onset Alzheimer Disease and its variants. Contin Minneap Minn. 2019;25(1):34–51.
2. Marshall GA, Fairbanks LA, Tekin S, Vinters HV, Cummings JL. Early-Onset Alzheimer's disease is Associated with Greater Pathologic Burden. J Geriatr Psychiatry Neurol. 2007;20(1):29–33.
3. Aziz AL, Giusiano B, Joubert S, Duprat L, Didic M, Gueriot C, et al. Difference in imaging biomarkers of neurodegeneration between early and late-onset amnestic Alzheimer's disease. Neurobiol Aging. 2017;54:22–30.
4. Polsinelli AJ, Logan PE, Lane KA, Manchella MK, Nemes S, Sanjay AB et al. APOE ε4 carrier status and sex differentiate rates of cognitive decline in early- and late-onset Alzheimer's disease. Alzheimers Dement [Internet]. 2023 [cited 2023 Apr 24];n/a(n/a). https://doi.org/10.1002/alz.12831
5. Spina S, La Joie R, Petersen C, Nolan AL, Cuevas D, Cosme C, et al. Comorbid neuropathological diagnoses in early versus late-onset Alzheimer's disease. Brain J Neurol. 2021;144(7):2186–98.
6. Tanner JA, Iaccarino L, Edwards L, Asken BM, Gorno-Tempini ML, Kramer JH et al. Amyloid, tau and metabolic PET correlates of cognition in early and late-onset Alzheimer's disease. Brain. 2022;awac229.
7. Hammers DB, Eloyan A, Taurone A, Thangarajah M, Beckett L, Gao S et al. Profiling baseline performance on the Longitudinal Early-Onset Alzheimer's Disease Study (LEADS) cohort near the midpoint of data collection. Alzheimers Dement [Internet]. 2023 May 31 [cited 2023 Sep 5];n/a(n/a). https://doi.org/10.1002/alz.13160
8. H C, S J, SJ K, JM L, JH L, GH K, et al. Longitudinal changes of cortical thickness in early- versus late-onset Alzheimer's disease. Neurobiol Aging. 2013;34(7):e19219–192115.
9. Hamelin L, Bertoux M, Bottlaender M, Corne H, Lagarde J, Hahn V, et al. Sulcal morphology as a new imaging marker for the diagnosis of early onset Alzheimer's disease. Neurobiol Aging. 2015;36(11):2932–9.
10. Migliaccio R, Agosta F, Possin KL, Canu E, Filippi M, Rabinovici GD, et al. Mapping the progression of atrophy in early- and late-onset Alzheimer's Disease. J Alzheimers Dis JAD. 2015;46(2):351–64.
11. Squire LR, Zola-Morgan S. The medial temporal lobe memory system. Science. 1991;253(5026):1380–6.
12. Eichenbaum H, Otto T, Cohen NJ. Two functional components of the hippocampal memory system. Behav Brain Sci. 1994;17(3):449–72.
13. Ritchey M, Libby LA, Ranganath C. Cortico-hippocampal systems involved in memory and cognition: the PMAT framework. Prog Brain Res. 2015;219:45–64.
14. Braak H, Braak E. Neuropathological stageing of Alzheimer-related changes. Acta Neuropathol (Berl). 1991;82(4):239–59.
15. Llamas-Rodríguez J, Oltmer J, Greve DN, Williams E, Slepneva N, Wang R, et al. Entorhinal Subfield vulnerability to Neurofibrillary tangles in Aging and the preclinical stage of Alzheimer's Disease. J Alzheimers Dis. 2022;87(3):1379–99.
16. Wisse LEM, Ravikumar S, Ittyerah R, Lim S, Lane J, Bedard ML, et al. Downstream effects of polypathology on neurodegeneration of medial temporal lobe subregions. Acta Neuropathol Commun. 2021;9(1):128.
17. Knopman DS, Amieva H, Petersen RC, Chételat G, Holtzman DM, Hyman BT, et al. Alzheimer disease. Nat Rev Dis Primer. 2021;7(1):33.
18. Rabinovici GD, Carrillo MC, Forman M, DeSanti S, Miller DS, Kozauer N, et al. Multiple comorbid neuropathologies in the setting of Alzheimer's disease neuropathology and implications for drug development. Alzheimers Dement Transl Res Clin Interv. 2017;3(1):83–91.
19. Palmqvist S, Rossi M, Hall S, Quadalti C, Mattsson-Carlgren N, Dellavalle S, et al. Cognitive effects of Lewy body pathology in clinically unimpaired individuals. Nat Med. 2023;29(8):1971–8.
20. Tosun D, Yardibi O, Benzinger TLS, Kukull WA, Masters CL, Perrin RJ et al. Identifying individuals with non-Alzheimer's disease co-pathologies: A precision medicine approach to clinical trials in sporadic Alzheimer's disease. Alzheimers Dement [Internet]. 2023 Sep 4 [cited 2023 Nov 1];n/a(n/a). https://doi.org/10.1002/alz.13447
21. Kapasi A, DeCarli C, Schneider JA. Impact of multiple pathologies on the threshold for clinically overt dementia. Acta Neuropathol (Berl). 2017;134(2):171–86.
22. Nelson PT, Dickson DW, Trojanowski JQ, Jack CR, Boyle PA, Arfanakis K, et al. Limbic-predominant age-related TDP-43 encephalopathy (LATE): consensus working group report. Brain. 2019;142(6):1503–27.
23. Palmqvist S, Janelidze S, Quiroz YT, Zetterberg H, Lopera F, Stomrud E, et al. Discriminative accuracy of plasma Phospho-tau217 for Alzheimer Disease vs Other Neurodegenerative disorders. JAMA. 2020;324(8):772–81.
24. Connor DJ, Sabbagh MN. Administration and Scoring Variance on the ADAS-Cog. J Alzheimers Dis. 2008;15(3):461–4.
25. Hansson O, Seibyl J, Stomrud E, Zetterberg H, Trojanowski JQ, Bittner T, et al. CSF biomarkers of Alzheimer's disease concord with amyloid-β PET and predict clinical progression: a study of fully automated immunoassays in BioFINDER and ADNI cohorts. Alzheimers Dement. 2018;14(11):1470–81.
26. Hansson O, Batrla R, Brix B, Carrillo MC, Corradini V, Edelmayer RM, et al. The Alzheimer's Association international guidelines for handling of cerebrospinal fluid for routine clinical measurements of amyloid β and tau. Alzheimers Dement. 2021;17(9):1575–82.
27. Janelidze S, Stomrud E, Brix B, Hansson O. Towards a unified protocol for handling of CSF before β-amyloid measurements. Alzheimers Res Ther. 2019;11(1):63.
28. Gobom J, Parnetti L, Rosa-Neto P, Vyhnalek M, Gauthier S, Cataldi S et al. Validation of the LUMIPULSE automated immunoassay for the measurement of core AD biomarkers in cerebrospinal fluid. 2022;60(2):207–19.
29. Pichet Binette A, Franzmeier N, Spotorno N, Ewers M, Brendel M, Biel D, et al. Amyloid-associated increases in soluble tau relate to tau aggregation rates and cognitive decline in early Alzheimer's disease. Nat Commun. 2022;13(1):6635.
30. Folstein MF, Folstein SE, McHugh PR. Mini-mental state: a practical method for grading the cognitive state of patients for the clinician. J Psychiatr Res. 1975;12(3):189–98.
31. Lezak MD. Neuropsychological assessment. [Internet]. 5. ed. Oxford University Press; 2012. http://ludwig.lub.lu.se/login?url=https://search.ebscohost.com/login.aspx?direct=true&db=cat07147a&AN=lub.4785165&site=eds-live&scope=site
32. Mack WJ, Freed DM, Williams BW, Henderson VW. Boston naming test: shortened versions for Use in Alzheimer's Disease. J Gerontol. 1992;47(3):P154–8.
33. Reitan RM. Validity of the trail making test as an Indicator of Organic Brain damage. Percept Mot Skills. 1958;8(3):271–6.
34. Smith A. Symbol digit modalities test. Western psychological services Los Angeles; 1973.
35. Warrington EK, James M, Thames Valley Test Company. The visual object and space perception battery. Bury St. Edmunds: Thames Valley Test Company Bury St. Edmunds; 1991.
36. Berron D, Vieweg P, Hochkeppler A, Pluta JB, Ding SL, Maass A, et al. A protocol for manual segmentation of medial temporal lobe subregions in 7Tesla MRI. NeuroImage Clin. 2017;15:466–82.
37. Xie L, Wisse LEM, Pluta J, de Flores R, Piskin V, Manjón JV, et al. Automated segmentation of medial temporal lobe subregions on in vivo T1-weighted MRI in early stages of Alzheimer's disease. Hum Brain Mapp. 2019;40(12):3431–51.
38. Xie L, Wisse LEM, Wang J, Ravikumar S, Khandelwal P, Glenn T, et al. Deep label fusion: a generalizable hybrid multi-atlas and deep convolutional neural network for medical image segmentation. Med Image Anal. 2023;83:102683.
39. Yushkevich PA, Pluta JB, Wang H, Xie L, Ding SL, Gertje EC, et al. Automated volumetry and regional thickness analysis of hippocampal subfields and medial temporal cortical structures in mild cognitive impairment. Hum Brain Mapp. 2015;36(1):258–87.
40. de Flores R, Wisse LEM, Das SR, Xie L, McMillan CT, Trojanowski JQ, et al. Contribution of mixed pathology to medial temporal lobe atrophy in Alzheimer's disease. Alzheimers Dement. 2020;16(6):843–52.
41. Touroutoglou A, Katsumi Y, Brickhouse M, Zaitsev A, Eckbo R, Aisen P et al. The Sporadic Early-onset Alzheimer's Disease Signature Of Atrophy: Preliminary Findings From The Longitudinal Early-onset Alzheimer's Disease Study

(LEADS) Cohort. Alzheimers Dement [Internet]. 2023 Oct 18 [cited 2023 Nov 8];n/a(n/a). https://doi.org/10.1002/alz.13466
42. Leuzy A, Smith R, Ossenkoppele R, Santillo A, Borroni E, Klein G, et al. Diagnostic performance of RO948 F 18 Tau Positron Emission Tomography in the differentiation of Alzheimer Disease from Other Neurodegenerative disorders. JAMA Neurol. 2020;77(8):955–65.
43. Baker SL, Maass A, Jagust WJ. Considerations and code for partial volume correcting [18F]-AV-1451 tau PET data. Data Brief. 2017;15:648–57.
44. Rousset OG, Ma Y, Evans AC. Correction for partial volume effects in PET: principle and validation. J Nucl Med. 1998;39(5):904–11.
45. Cho H, Choi J, Hwang M, Kim Y, Lee H, Lee H, et al. In vivo cortical spreading pattern of tau and amyloid in the Alzheimer Disease Spectrum. Ann Neurol. 2016;80(2):247–58.
46. Leuzy A, Smith R, Cullen NC, Strandberg O, Vogel JW, Binette AP, et al. Biomarker-based prediction of longitudinal tau Positron Emission Tomography in Alzheimer Disease. JAMA Neurol. 2022;79(2):149–58.
47. Cerri S, Puonti O, Meier DS, Wuerfel J, Mühlau M, Siebner HR, et al. A contrast-adaptive method for simultaneous whole-brain and lesion segmentation in multiple sclerosis. NeuroImage. 2021;225:117471.
48. Puonti O, Iglesias JE, Van Leemput K. Fast and sequence-adaptive whole-brain segmentation using parametric bayesian modeling. NeuroImage. 2016;143:235–49.
49. R Core Team. R: a language and environment for statistical computing. Vienna, Austria: R Foundation for Statistical Computing; 2020.
50. Chishiki Y, Hirano S, Li H, Kojima K, Nakano Y, Sakurai T, et al. Different patterns of Gray Matter volume reduction in early-onset and late-onset Alzheimer Disease. Cogn Behav Neurol off J Soc Behav Cogn Neurol. 2020;33(4):253–8.
51. Lee EC, Kang JM, Seo S, Seo HE, Lee SY, Park KH, et al. Association of Subcortical Structural shapes with tau, amyloid, and cortical atrophy in early-onset and late-onset Alzheimer's Disease. Front Aging Neurosci. 2020;12:563559.
52. Ossenkoppele R, Mattsson N, Teunissen CE, Barkhof F, Pijnenburg Y, Scheltens P, et al. Cerebrospinal fluid biomarkers and cerebral atrophy in distinct clinical variants of probable Alzheimer's Disease. Neurobiol Aging. 2015;36(8):2340–7.
53. Visser D, Verfaillie SCJ, Wolters EE, Coomans EM, Timmers T, Tuncel H, et al. Differential associations between neocortical tau pathology and blood flow with cognitive deficits in early-onset vs late-onset Alzheimer's disease. Eur J Nucl Med Mol Imaging. 2022;49(6):1951–63.
54. Smith R, Strandberg O, Mattsson-Carlgren N, Leuzy A, Palmqvist S, Pontecorvo MJ, et al. The accumulation rate of tau aggregates is higher in females and younger amyloid-positive subjects. Brain. 2020;143(12):3805–15.
55. Tort-Merino A, Falgàs N, Allen IE, Balasa M, Olives J, Contador J, et al. Early-onset Alzheimer's disease shows a distinct neuropsychological profile and more aggressive trajectories of cognitive decline than late-onset. Ann Clin Transl Neurol. 2022;9(12):1962–73.
56. Zhu XC, Tan L, Wang HF, Jiang T, Cao L, Wang C et al. Rate of early onset Alzheimer's disease: a systematic review and meta-analysis. Ann Transl Med Vol 3 No 3 March 10 2015 Ann Transl Med [Internet]. 2015 [cited 2015 Jan 1]; https://atm.amegroups.org/article/view/5826

Publisher's note